

Numerical Simulation of Heavy Rainfall Case in South Asia

Rasul, G¹, Q. Z. Chaudhry¹ and A. Mahmood¹

Abstract

The heavy monsoon precipitation over the Indus plains of south Asia was examined by non-hydrostatic numerical model MM5. Model-simulated rainfall over Karachi and its surrounding area during 27-29 July 2003 was compared with the observations, and the relationships between this heavy rainfall process and large scale circulations, such as the westerly jet, low-level jet, vertical wind speed and water vapour transport were analyzed to further understand the mechanisms for simulating heavy rainfall. The analyses results show that (1) the mentioned above model can reproduce the pattern of heavy precipitation over southern plains of south Asia effectively but rain belts are shifted slightly southwards. (2) The simulated Sub-tropical High (STH) that controls the cold air advections from northern latitudes to southern latitudes in mid troposphere is stronger than observation and is extended eastward, which possibly leads to southward shift of heavy rain belt. (3) The westerly jet at 200 hPa and low-level jet at 850 hPa, both of which are related to the heavy monsoon precipitation, are reasonably reproduced by MM5, although the intensity of simulated low-level jet is stronger and orientation shows northwest leaning which, in addition to STH strength, may be the cause of MM5 producing quantitatively much higher rainfall as compared to observed precipitation.

Introduction

South Asian summer is characterized by frequent mesoscale convective developments sometimes in the form of dry thunderstorms/dust storms under insufficient moisture conditions and heavy precipitation in case of optimal moisture supply. Later half of July and first half of August is the peak of monsoon season with more frequent showers along Himalayan range but occasional rains over the southern plain. Heavy precipitations of more than 50mm are more common along high elevation windward plain of Pakistan and India. However, occurrence of such cases is rare over arid plains of southwestern India and southeastern parts of Pakistan. Minimal probability of occurrence of heavy rain in these area leads to unpreparedness which poses a threat of severe damages if such event takes place. Heavy downpour over southeastern parts of Pakistan during 25-28 July 2003 was such a rare weather event because of the length of wet spell and resultant flooding that occurred across Karachi metropolitan and adjoining townships.

Examination of observational data along with satellite and radar imageries revealed that the flooding was produced by combined multiple Mesoscale Convective Systems (MCSs). The convection cells developed and organized over western Rajasthan, the province of India adjoining Pakistan's Sindh province sharing southern borders. A well-marked low-pressure system existing over the Bay of Bengal also developed into monsoon depression on the same day (24 July 2003) and moved westward. The monsoon depression, although lost much of intensity during its land journey but it was still an intense low-pressure system having a potential to produce heavy downpour under any trigger action. Both the systems combined with each other on 27 July 2003 over Southeastern parts of Pakistan providing the trigger to stormy weather in the area. Prior to the interaction during the four days period, MCSs followed a diurnal cycle of dissipation and reorganization. Analysis of 1200UTC data shows that the convection initiated in a region of weak upper level divergent flow. Moderate convective instability and vertical wind shear across the region resulted into multicellular structure of clouds under adequate moisture advection. In addition, the convective systems after interaction with weakening monsoon depression appeared to move along almost east-west oriented outflow boundary during the morning resulting in heavy rainfall over Karachi metropolitan area.

Das et al (2002) performed a comparative study of performance of two numerical models and simulated a heavy rainfall episode in last pentad of June 2002 over some areas of the west coast of India. They stated

¹ Pakistan Meteorological Department

that the T80 global forecast model of National Center for Medium Range Weather Forecasting (NCMRWF) was unable to forecast successfully the intensity of the rainfall as observed. A high-resolution mesoscale model (MM5) was also used to reproduce different fields for the same case. They elaborated that the mesoscale model (MM5) forecasted a better distribution of rainfall than the NCMRWF model, however, sometimes the location of maximum rainfall is misplaced as compared to observations. Gao et al. (2002) analyzed the moist potential vorticity anomaly with heat and mass forcing in torrential rain systems by numerical simulation. Gao et al. (2005a, 2005b, 2002006) performed a cloud-resolving model simulation to study the surface rainfall processes, the moist and dynamic vorticity vectors associated with two-dimensional tropical convection, and the impacts of ice microphysics on rainfall and thermodynamic processes in the tropical deep convective regime. Yang et al. (2008) simulated the asymmetric structure of the landfalling typhoon “Haitang”.

In order to grasp the intensity and structure of heavy rainfall occurring on 28 July 2003, the PSU-NCAR three-dimensional, non-hydrostatic mesoscale model (MM5 version3) is used for the present study. The areas of precipitation and clouds are introduced into the initial model data through subjective analysis of satellite and radar observations. Preliminary analysis of the simulations revealed that the numerical model captured several qualitative details of the rainfall event.

Section 2 describes briefly the basic features as well as characteristics of the MM5 model used in the numerical simulation of heavy rain event. The observed synoptic conditions leading to the heavy rainfall episode were compared with simulated model outputs for testing the ability of model to reproduce the actual conditions in the section 3. Finally, the results and conclusions are presented in the section 4 and 5.

MM5 Model Configuration

The MM5 model is a 5th generation PSU/NCAR Mesoscale Model (limited area), non-hydrostatic, terrain-following sigma coordinate, designed to simulate or predict mesoscale & regional scale atmospheric circulation (Dudhia et al., 2002). The model has been adapted for real time mesoscale weather forecasting at NCMRWF (Das, 2002). The model uses the Grell scheme (Grell et al., 1994) for cumulus parameterization and, a non-local closure scheme for boundary layer parameterization. Explicit treatment of cloud water, rainwater, snow water and ice has been performed using the simple ice scheme of Dudhia (1996). Cloud radiation interaction is allowed between explicit cloud and clear air (IFRAD=2).

A two-way interactive nested grid system is used to include three domains. They consist of a 45-km grid domain (D01, 100×100 grid points), a 15-km grid domain (D02, 121×121 grid points). The model top is located at 100 hPa. The 23 vertical sigma levels are 1, 0.99, 0.98, 0.96, 0.93, 0.89, 0.85, 0.75, 0.7, 0.65, 0.6, 0.55, 0.5, 0.45, 0.4, 0.35, 0.3, 0.25, 0.2, 0.15, 0.1, 0.05, 0.0. The presentation will focus on the results for the 45-km grid domain.

The microphysics for explicit moisture processes is treated using the mixed-phase microphysics scheme of Reisner et al. (1998), in which five prognostic equations are solved for mixing ratios of water vapor, cloud water, rainwater, cloud ice, and snow. The cumulus parameterization scheme of Grell (Grell et al. 1991) is employed for sub grid-scale convection in coarse grids. Blackadar’s high-resolution scheme (Blackadar 1979; Zhang and Anthes 1982) is adopted to calculate the turbulent fluxes in the PBL. Physics options for the 15-km grid simulations are the same as the coarse-grid simulation.

Model Initialization

6-hourly global analyses (27Jul0000UTC-28Jul0000UTC) with 1°×1° resolution from National Centers for Environmental Prediction (NCEP) are interpolated horizontally to model grid points. Then the standard upper air and surface observations are analyzed using a successive correction scheme on the base of first guess. No balancing between mass and wind fields is performed. Finally, the analyses are interpolated to the model levels. The numerical integration starts at 0000 UTC 25 July 2003. The time-dependent lateral boundary conditions are obtained by interpolating the 6-h observational analyses linearly in time. No other special observations are available for the present

case. Thus, it may be a serious challenge for the model to simulate the initiation and evolution of the convection band using only conventional observation data. The simulated results reveal that the numerical model captures several qualitative details of the heavy rainfall event quite reasonably.

Data for Validation and Method

The data set for validation contains both station data and grided data. The daily precipitation data are collected from several meteorological observatories of India and Pakistan. Over the region, 12-hourly $1^\circ \times 1^\circ$ zonal (u) and meridional (v) wind components (unit: ms^{-1}), geopotential height (unit: gpm), air temperature (unit: $^\circ\text{C}$) and relative humidity (unit: %) from the NCEP reanalysis dataset used to calculate the derived parameters which can not be directly observed by meteorological instruments. Among these derived parameters are specific humidity, vorticity, convergence, pseudo-equivalent potential temperature and the divergence of moisture flux.

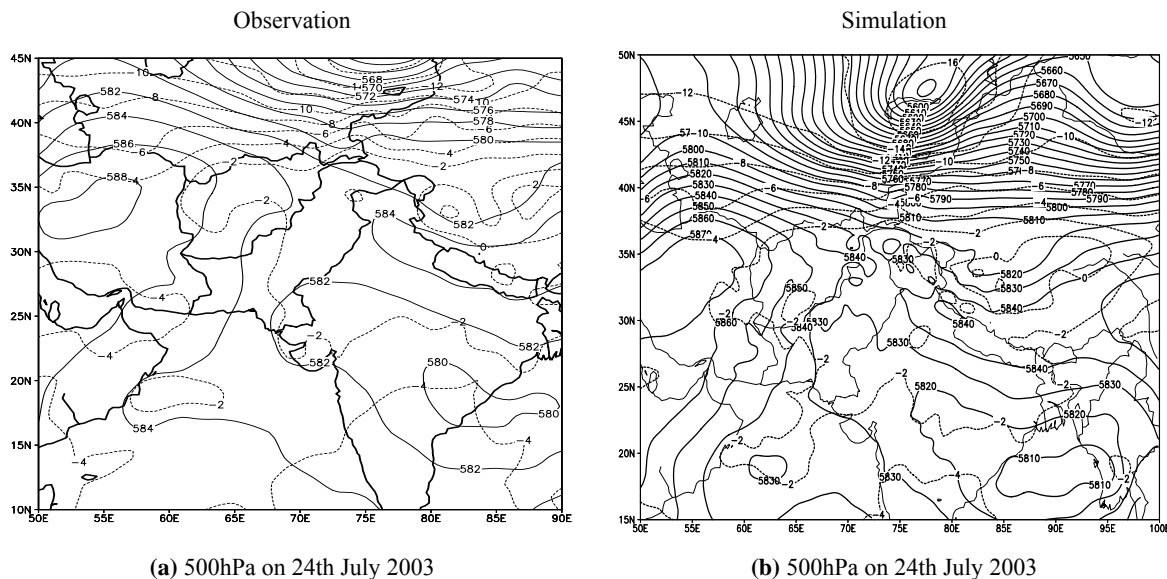
The westerly jet (also known as the upper level jet) is defined as existing when the wind speed is greater than 60 ms^{-1} , and the critical value of 14 ms^{-1} is used for the low level jet (Ding, 1991; Zhai, 1999). Instead of considering vertical profile to locate the upper level jet, wind speed field at 200hPa is drawn to identify the geographical location of the jet. Similarly wind speed analysis at 850hPa is presented to mark low-level jet.

Results and Discussion

Model output on various derived parameters is compared with their respective observed fields. They are presented and discussed in the following sections one by one.

Geopotential Height and Temperature Field

In figure 1, the geopotential heights and temperature fields at 500hPa are presented as observed and simulated by MM5 at formation (24th July) and interaction (28th July) stage. In presented domain, which represents mainly South Asian region, three planetary scale circulations can be seen clearly. They are (1) the western part of the STH (Sub-Tropical High), illustrated by 5880gpm contour prevailing over central Iran; (2) the mid-latitude trough of westerly wave extending down to 40°N across north of Pakistan; and (3) the low over the Bay of Bengal extending westward over central India into southeastern parts of Pakistan on 24th July.



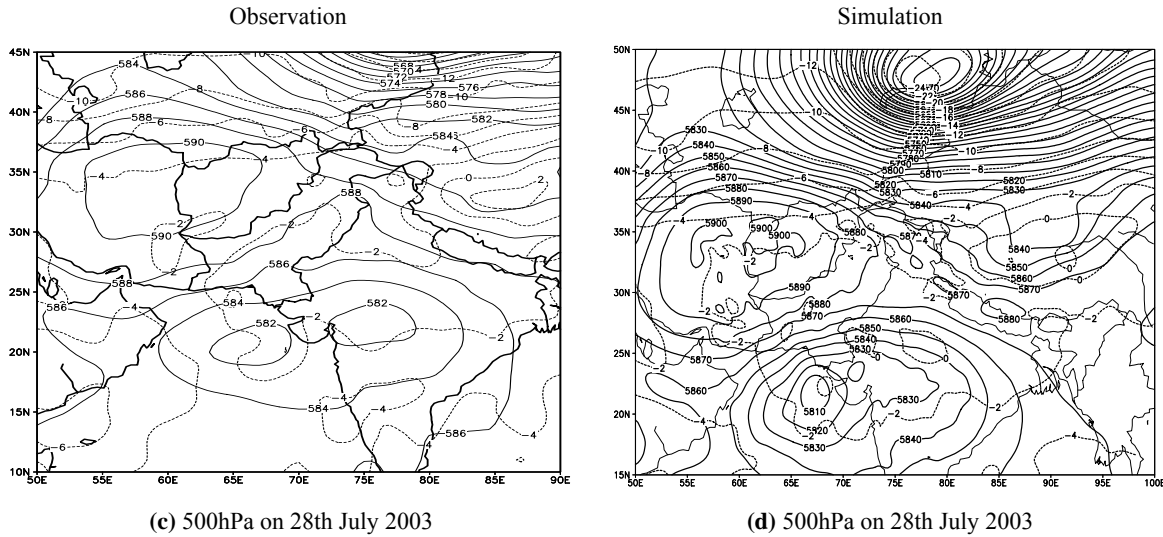


Fig 1: Observed and predicted Geopotential Height (gpm) and Temperature (C°) fields at 500hPa during the formation stage (a) on 24th July of meso-scale low over southeastern parts of Pakistan and adjoining parts of India as well as monsoon depression over the Bay of Bengal. On 28th July, both the systems interacted (b) over southeastern parts of Pakistan.

Later on it moved westward and then merged with a low over southeast Pakistan. Near center of the mid latitude low over 45°N, isotherm of -16°C were found whereas troughing down to 40°N bears -6°C in both the observed fields. Isotherm bearing value of -2°C mainly prevailed over India and Pakistan.

The simulated geopotential height pattern agrees with the observations except showing complete merger of meso-scale low and monsoon depression against their independent status in observed field on 28th July 2003. A minor deviation in the observed and simulated thermal regimes could be seen over Tibet Plateau where model predicted 2°C colder than the observed field.

Convergence and Vorticity

Both observed and simulated convergence fields at 500hPa at the formation and interaction stages are presented in Fig. 2. The area where convergence is taking place is represented by dotted lines whereas bold lines show divergence. In observed fields shown in Figure 2, there are several cells of convergence and divergence of varying intensity spread all over the domain.

However, well-marked convergence zones on 24th July 2003 can be seen over the southeastern parts of Pakistan (25°N, 72°E) and the Bay of Bengal (23°N, 90°E).

Another strong convergence zone neighbouring divergence is located north of Pakistan (40°N, 78°E) marking the southern extent of the westerly wave's trough. Two isolated convergence cell at 500hPa representing interaction of both meso-scale systems existed southeast of Pakistan in the observed field on 28th July 2003. Divergence prevailed over Afghanistan and Iran throughout the life cycle of both the systems whereas atmosphere over the Tibet Plateau can be seen stable or even neutral.

The results produced by model are more or less consistent with observation regarding the formation of meso-scale low over southeastern parts of Pakistan and the monsoon depression over the Bay of Bengal. Similarly convergence across north of Pakistan and existence of divergence zones over Afghanistan and Iran are also confirmatory with observation. However, model produced strong convergence over Tibet Plateau during the life cycle, which is an exaggeration against the observed fields.

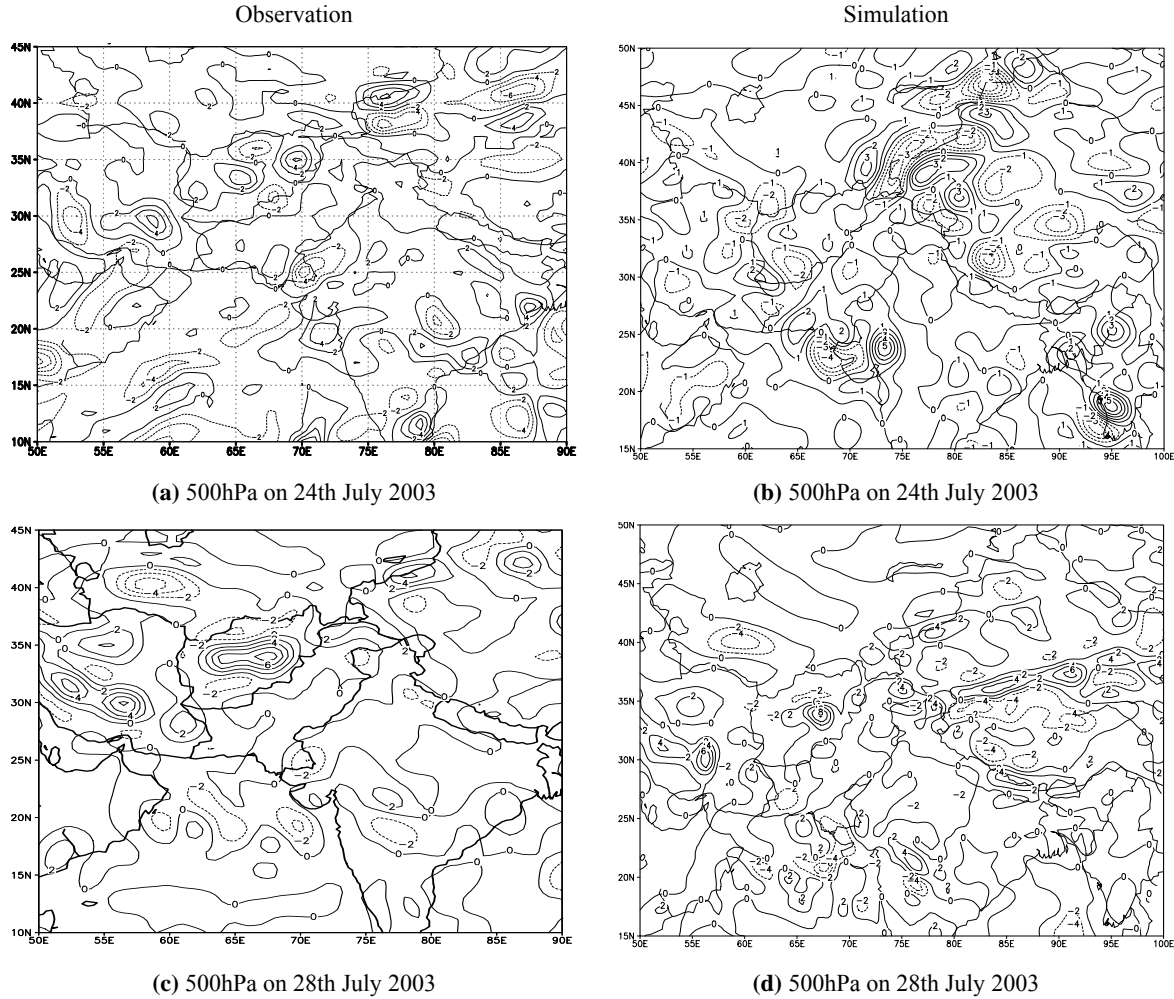


Fig 2: Convergence ($\times 10^{-1} \text{ S}^{-1}$) field at 500hPa (0000UTC) during formation stage (24th July 2003) and after interaction (28th July 2003). Convergence is represented by dotted isolines and divergence with bold lines.

Vorticity fields both observed and simulated at 500hPa for initial and final stages of the systems are presented in Figure 3. In observation field on 24th July 2003, positive vorticity zones are apparent over the origins of both the systems (see Fig 3a). Also a strong zone of positive vorticity sandwiched between two negative zones over Tibet Plateau can be seen. At the interaction stage on 28th July 2003, strong positive vorticity cells existing north south across land and sea boundary in the lower half of the domain represent both the systems. Another strong cell of positive vorticity lies in the upper half over north of Pakistan (Fig 3c).

The vorticity fields produced by MM5 differ from observation over the Bay of Bengal at the formation stage of monsoon depression on 24th July 2003 as shown in Figure 3a,b. In observed field, positive vorticity can be seen prevailing over North Bay of Bengal whereas model output shows negative vorticity dominant over the northern part of the Bay where a low pressure was transformed into a monsoon depression on 24th July. However, model simulation is in general agreement with formation of the meso-scale low over southeastern parts of Pakistan (Fig 3a,b) and the interaction stage of both the systems (Fig 3c,d).

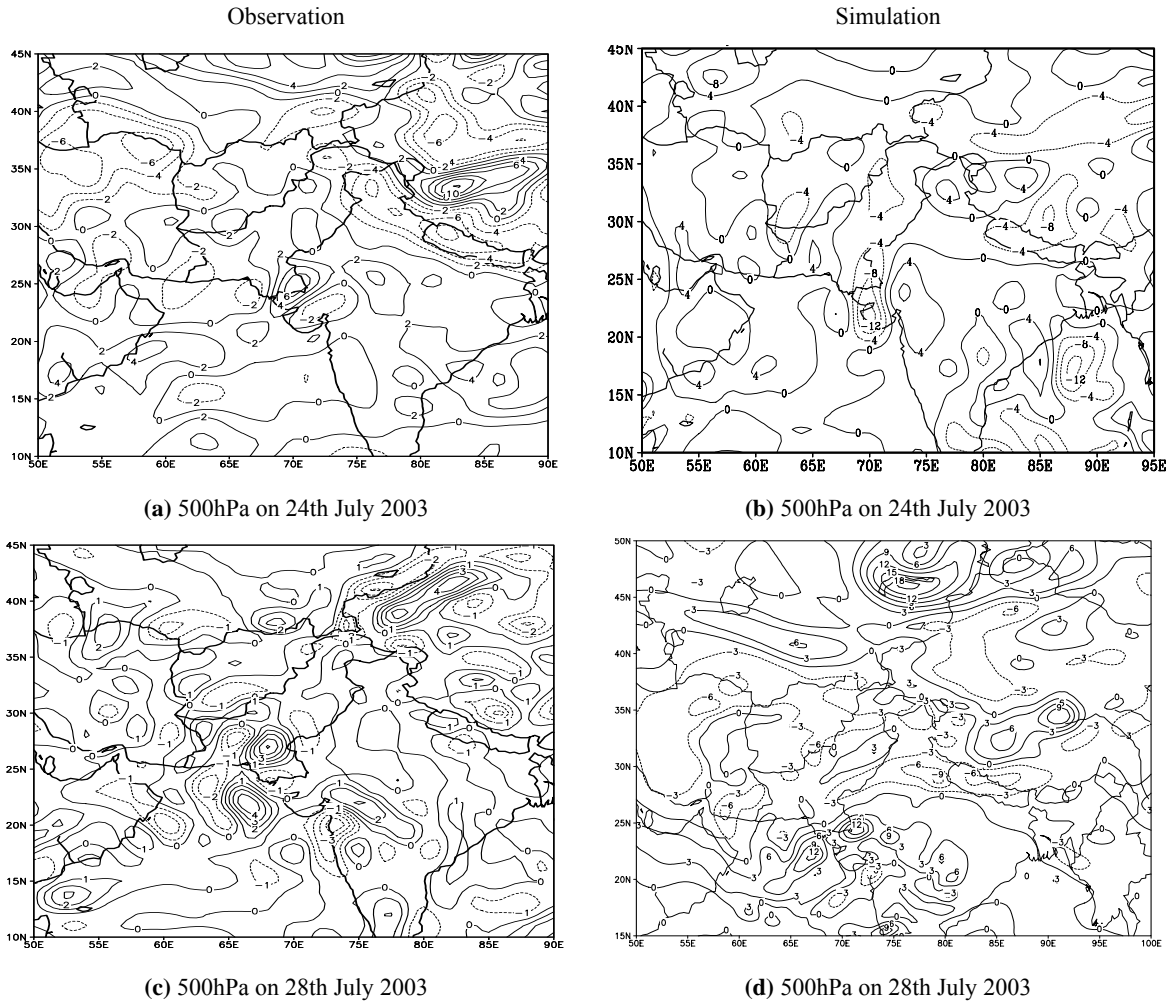


Fig 3: Vorticity Fields ($\times 10^{-5} \text{s}^{-1}$) at 500hPa (0000UTC) as observed and predicted by MM5 model. On 24th July, meso-scale low formed over southeastern parts Pakistan and adjoining India whereas formation of monsoon depression

Relative Humidity and Water Vapour Transport

Vertical profiles of relative humidity (%) along 68°E as observed and simulated from formation to merging stage of the systems are presented in Fig 4. In observed field on 25th July 2003, a saturated (100% RH) zone existed above 25°N from 700hPa to 450hPa whereas model produced field showed 70%-80% relative humidity there.

However, existence of relatively drier zone just north of 25°N (Karachi) near the surface as seen in observations on 25th and 28th July was well captured by the model. Similarly, model also produced the spread of saturated zone as observations depicted between 22°N and 26°N from surface to 400hPa (Fig 4a-d). However, the quantitative assessment of relative humidity values computed by the model, in general, remained 20% to 25% less than the observed values.

Convergence of the moisture flux in the model domain is shown in Fig 5. In observation and model-produced fields on 24th July, a strong convergence zone is existed at 25°N and 72°E that marks the formation of mesoscale low over that area. Over the Bay of Bengal, the birthplace of the monsoon depression, the convergence cells are neither organized in observation nor in the simulated field (Fig 5a,b). In the observation field, an extended trail of convergence cells could be seen along the east

coast of India whereas simulation presented such cells over the north Bay of Bengal with major concentration along the Myanmar coast. Not only they differ in geographical location but also in terms of their intensity. Another prominent feature is the strong convergence of moisture over southeastern Sindh and western Rajasthan in both the observed and simulated fields. Although model depicts some exaggeration over the observed convergence.

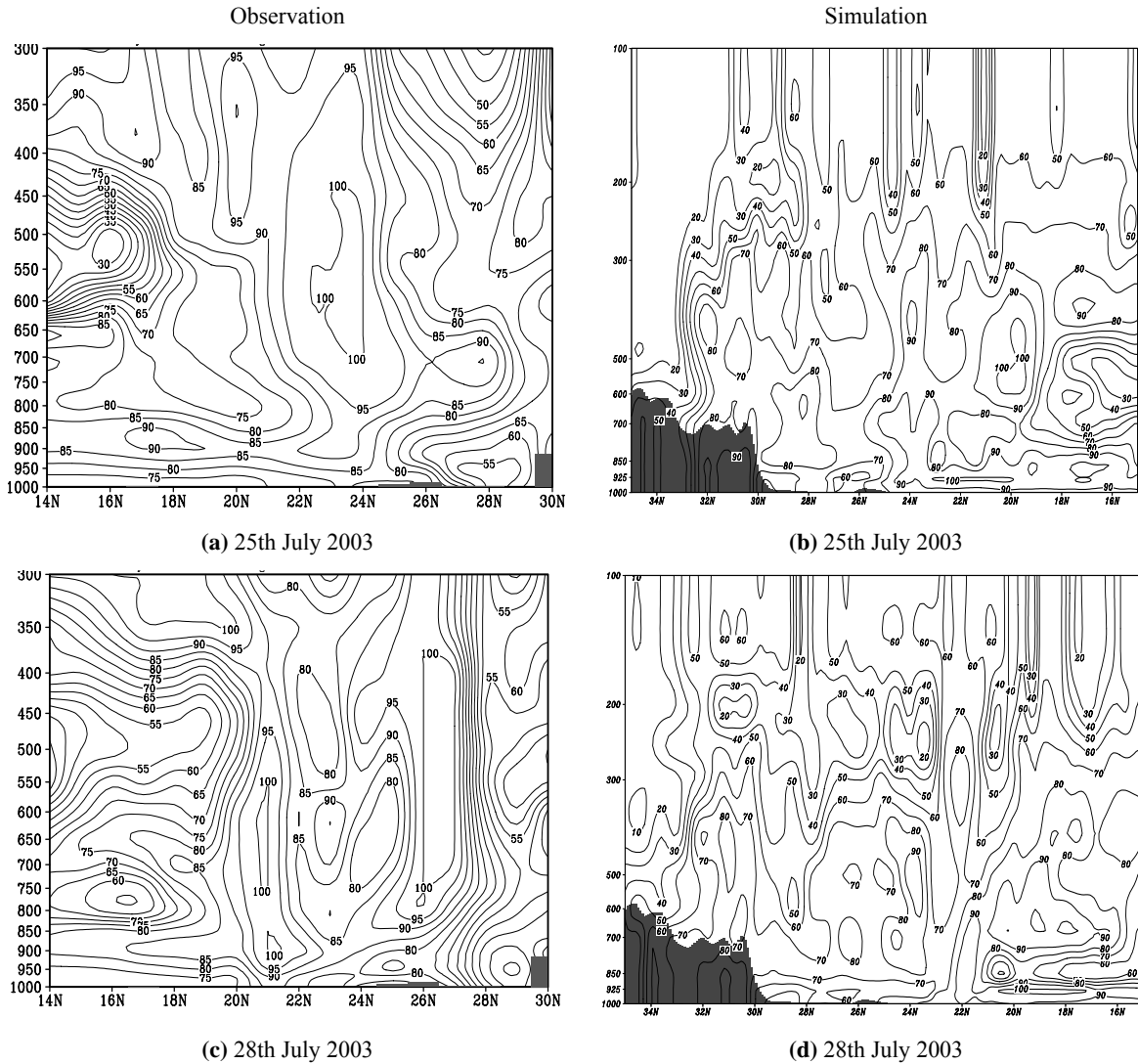


Fig 4: Vertical profile of relative humidity (%) as observed and predicted by MM5 along 68°E longitude passing east of Karachi (24°-54°). Formation of meso-scale low took place on 24th July 2003 and it merged with dissipating tropical depression on 28th July 2003 east of Karachi.

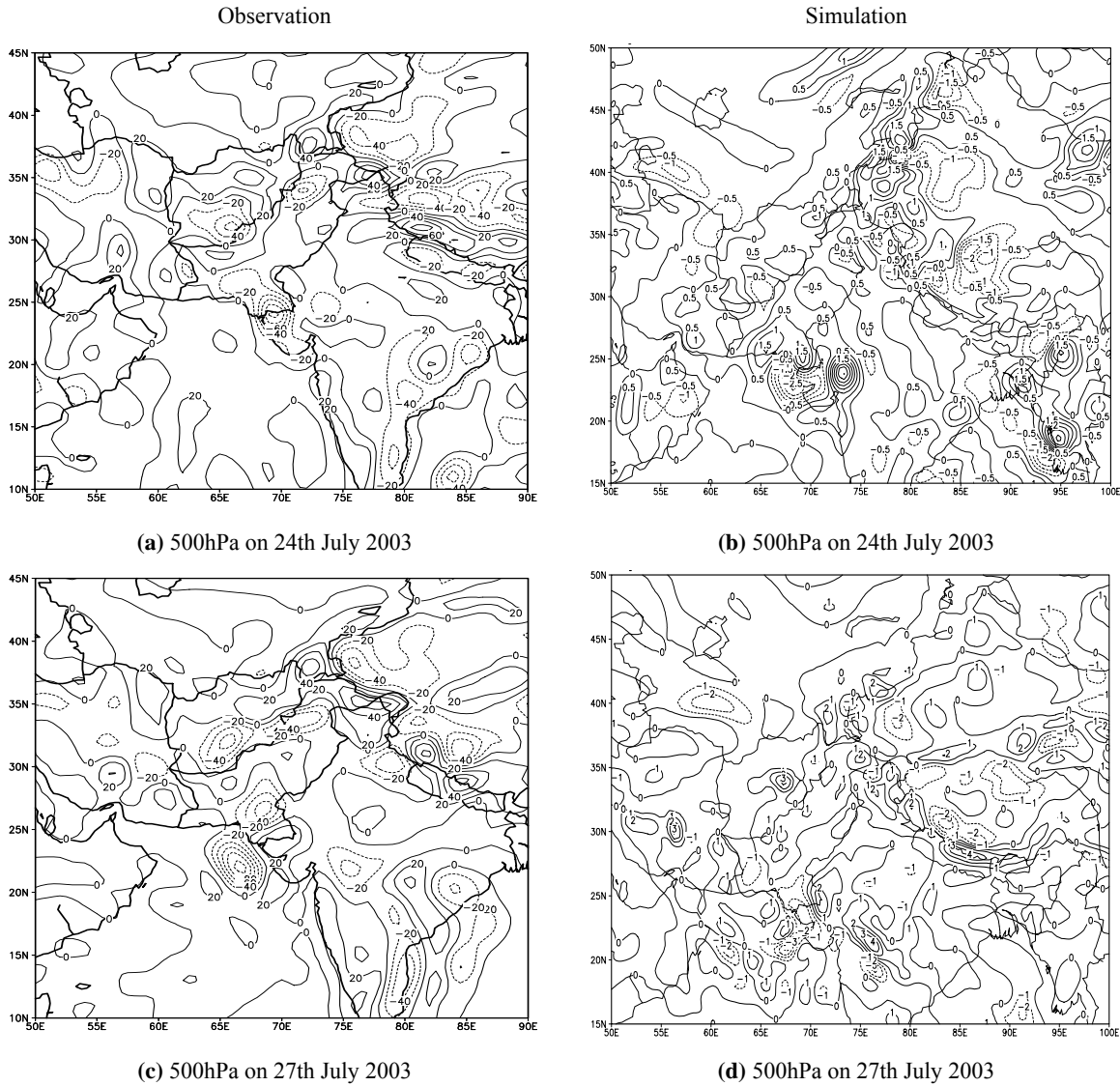


Fig 5: At 500hPa observed and simulated fields (0000UTC) of divergence of moisture flux (gm-ls-lhPa-l) at the formation stage and final stage of combination. Solid lines show divergence whereas dotted lines mention convergence zones.

Interaction of both the systems at 25°N and 68°E could be clearly seen (Fig5c,d) in the observed and simulated fields on 27th July 2003. Two isolated convergence cells of moisture flux are merging together along the coast of Arabian Sea neighbouring Karachi and a divergence zone is also located in the vicinity.

Streamline Fields

Streamlines are the most helpful tools to determine the moisture flow routes and the convergent and divergent centers in meteorological domains under investigation. Figure 6 illustrates the streamline fields at 850hPa and 700hPa at formation and combination stage. Two large-scale circulations could be seen in the observation: One is the ridge of the mid latitude anticyclone in the northern part of the

domain and another is in the tropics in the form of a monsoon depression over the Bay of Bengal and a meso-scale low over the southeastern part of Pakistan.

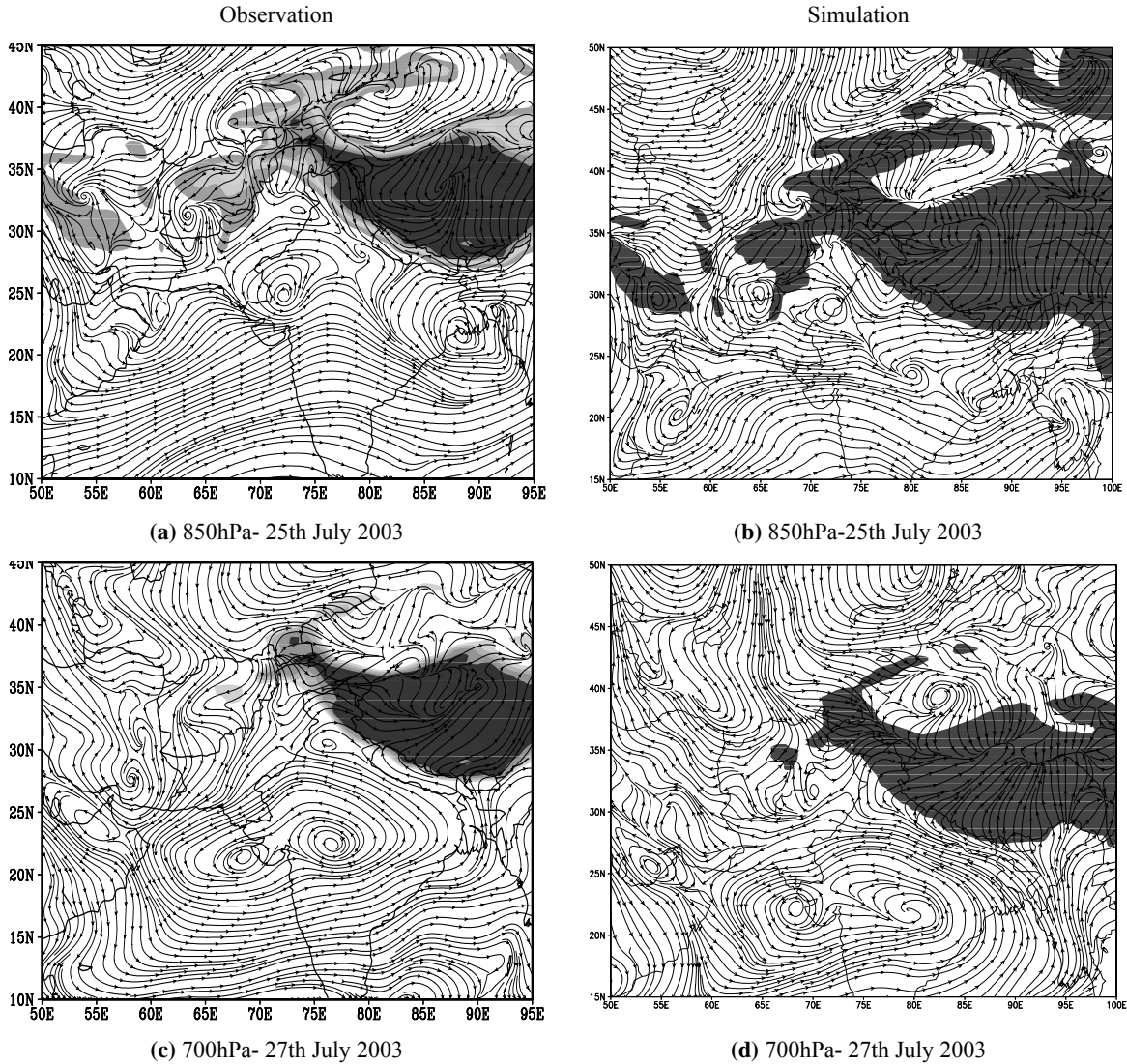


Fig 6: Observed and simulated Streamline fields at the inception and merger of both the interacting systems. (a) Observation at 700hPa (b) Simulated at 700hPa during developing stage and (c) Observation at 500hPa (d) Simulated at 500hPa during interaction.

The model reproduced both the observed large-scale circulations, though the position of the meso-scale low in 700hPa simulation is slightly shifted northward at the initial stage (Fig 6a,b). However, MM5 presented a true picture at 500hPa regarding the location as well as orientation of the systems both in the northern part of the domain and in the tropical belt. An active trough of mid latitude westerly wave extended down to north of Afghanistan followed by a strong ridge is also very well caught by the model (Fig 6c,d).

Pseudo-Equivalent Potential Temperature and Vertical Motion Field

The areas of convective instability may be identified by the pseudo-equivalent potential temperature and ascending motion. Observational facts of both the parameters were compared with the model output and presented in Fig 7 and 8. A vertical cross section along 68°E has been selected to study the

minor details of convective instability at the location where meso-scale low developed and both the systems combined together.

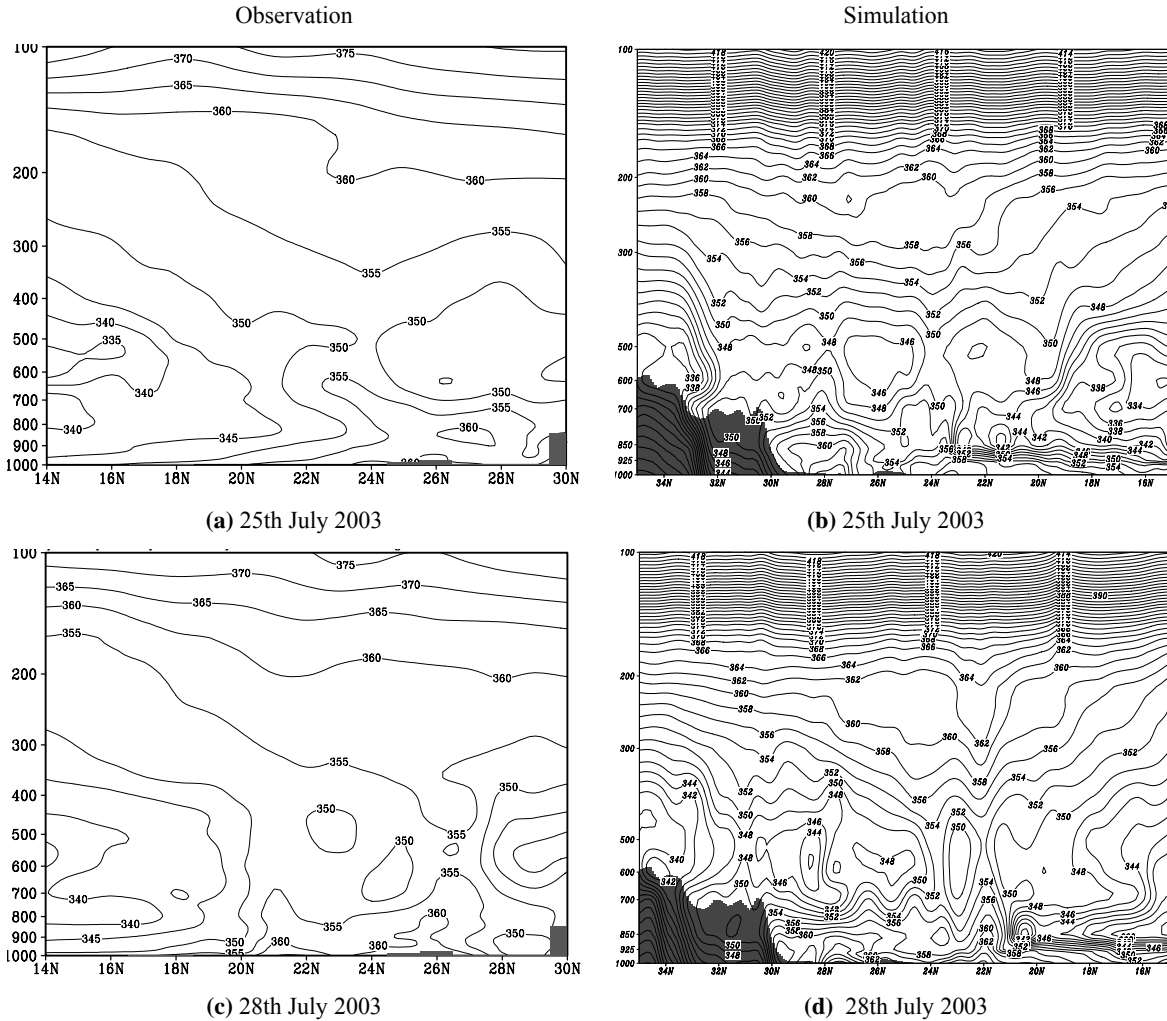


Fig 7: Observed and MM5 predicted vertical profiles of Pseudo-equivalent potential temperature (K) along 68°E longitude passing east of Karachi (24°-54'). Formation of meso-scale low took place on 24th July 2003 and it merged with dissipating monsoon depression on 28th July 2003 east of Karachi.

At the formation stage of the meso-scale low over southeastern part of Pakistan (25°N, 70°E), a zone of maximum pseudo-equivalent potential temperature existed from surface to 700hPa between 25°N and 28°N. Two minima prevailed in the domain. One existed above the maximum zone from 700hPa to 400hPa whereas another was observed little above surface to 400hPa (Fig 7a). The model reproduced the Pseudo-equivalent potential temperature successfully except a sharper gradient near the surface over the Indian Ocean south of Karachi as shown in Fig 7b.

On 28th July 2003, when the monsoon depression and the meso-scale low merged together, the maxima and minima which existed at the early stage of formation persisted with a little deviation in position. The model captured them reasonably well in agreement with their observational features. However, the strong maximum zone of pseudo-equivalent potential temperature near the surface above 21°N appeared in the model domain existed with a mild intensity in the observation field (Fig 7c,d).

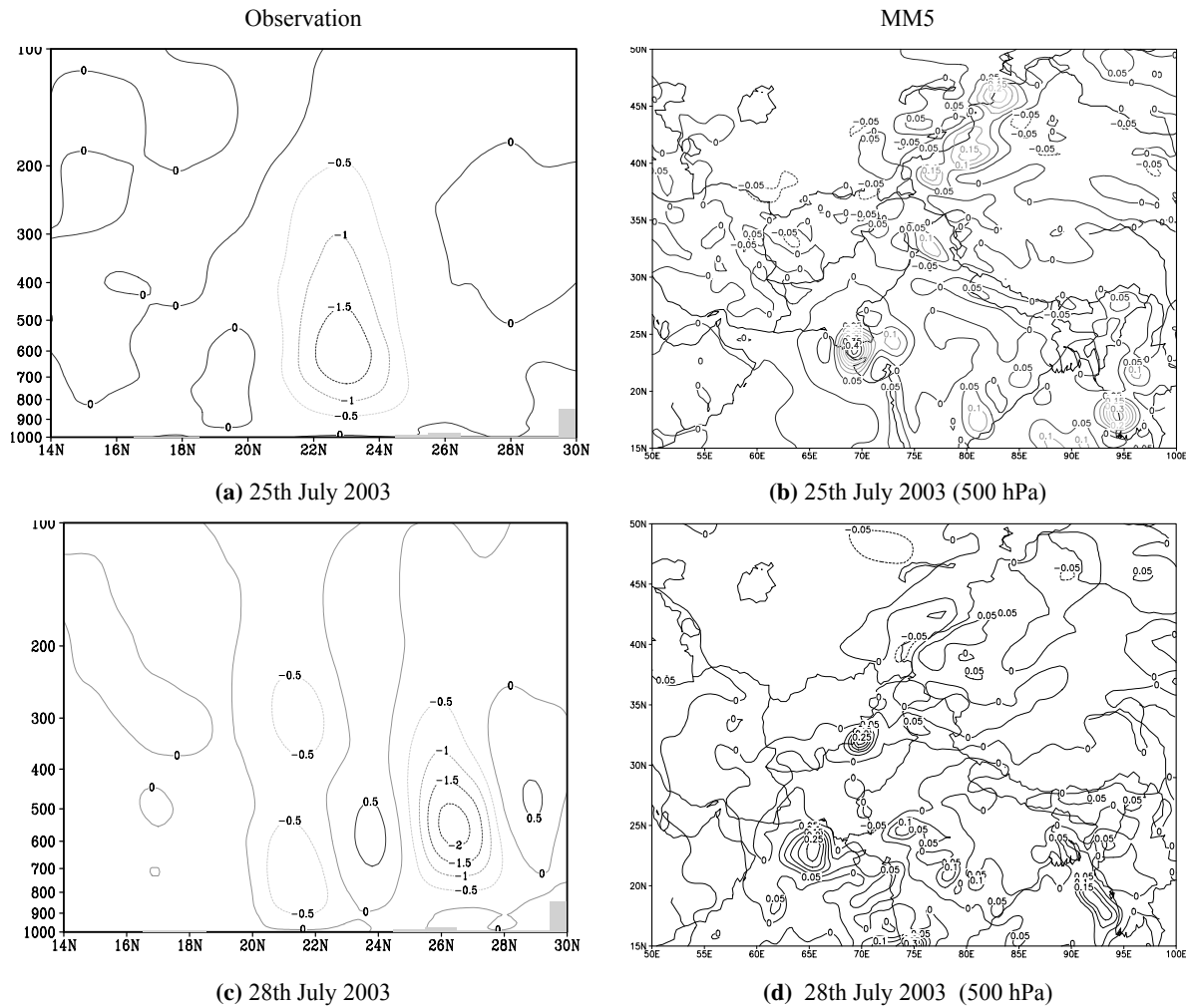


Fig 8: Observed Vertical profiles of vertical velocity (hPa.s⁻¹) along 68°E longitude to study the structural details of meso-scale low and MM5 output fields drawn for the formation and final stages. Dotted lines show upward motion.

In figure 8 (a & c), vertical profiles of ascending motion are presented along 68°E longitude at formation and merger stage. The vertical cross section covers only the meso-scale low formation on 25th July and merger of both the systems on 28th July. However, model domain covers surface features of both the systems initially developing over southeastern parts of Pakistan as well as on the Bay of Bengal and later on combining along the southeastern coastal belt of Pakistan. Strong upward motion from surface to mid-troposphere between 21°N and 25°N was observed on 25th July 2003 (Fig8a). Simulation results perfectly agreed with the observation.

Westerly and Low-Level Jets

Observed wind fields are drawn in Figure 9a and c at 850hPa as well as 200hPa to locate the low-level jet and westerly jet respectively at 0000UTC on 28 July 2003. For the low-level jet, the observed largest wind speed center shown in Figure 9a, is located along the west coast of India over the Arabian Sea with maximum wind speed of 20 ms⁻¹, and the simulated largest wind speed center perfectly coincided with the observed one with the maximum wind speed exceeding 22 ms⁻¹(shown in Fig 9b).

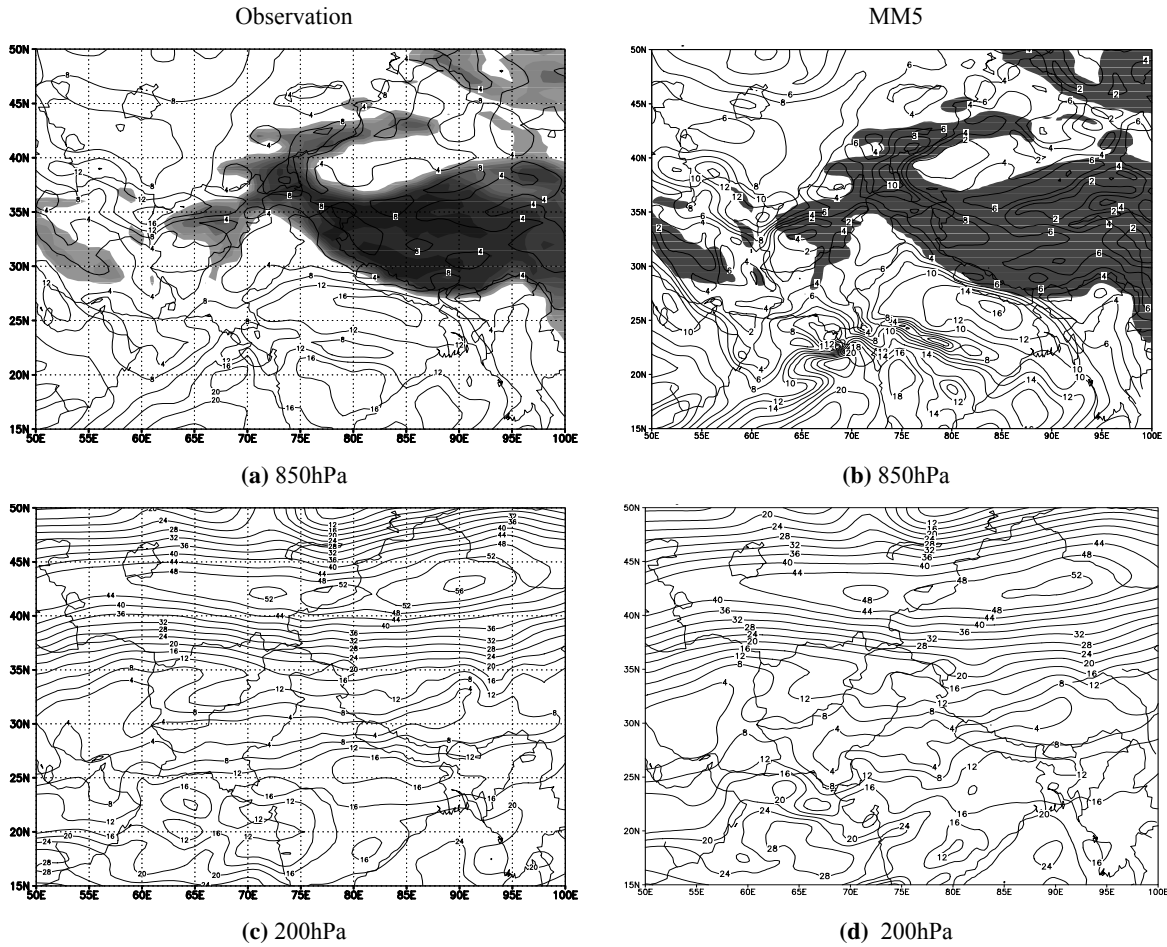


Fig 9: Observed and simulated low level Jet location at 850hPa wind chart (a) and (b) respectively drawn at 0000UTC on 28 July 2003. Westerly Jet in observed (c) and simulated (d) wind fields drawn simultaneously

The orientation of the observed and simulated low-level jet, however, differs slightly. The observed low-level jet is directed from the southwest to the northeast whereas simulated jet first takes southwest orientation and then turn northwest. However, both observed and simulated jets headed toward the maximum precipitation center.

For westerly jet, observations and simulations of wind speed at 200hPa of 0000UTC on 28 July 2003 are presented in Figure 9b and d. The observed and simulated maxima of wind speed in westerly jet is located north of China at 43°N and 90°E. Comparison shows that the simulated wind speed was slightly lower than the observed at the center i.e. 52ms⁻¹ compared with 56ms⁻¹. By and large, the location and orientation of jets in observed and simulated fields are in good agreement.

Rainfall Distribution

In Figure 10a, the observed total precipitation that occurred from 27 July 0000UTC to 28 July 0000UTC is presented. The simulated precipitation over the same period (Fig 10c) seems in good agreement with the observation except the main center in simulation is located south of the coastal belt of Pakistan over the Arabian Sea where observations are not available. The observed and simulated situation during next 24 hours is shown in Figure 10b and 10d respectively. The observational facts show that the system persisted along the coastal belt of Pakistan resulting in heavy downpour but the heavy rainfall belt in MM5 simulation seems to be located over the Arabian Sea off

the coast. It shows no precipitation over Karachi from 28 July 0000UTC to 29 July 0000UTC. Another heavy precipitation center can be seen over western Parts of India, which, however, exist in observation domain also. The simulated rainfall amounts are much higher than the observed values.

The model can reproduce the location of the observed heavy rainfall center head on to the low-level jet but near the westerly jet's wind speed maxima. The heavy rainfall belt with total precipitation over 200mm simulated by MM5 (see red shaded area in Fig 10c and 10d) is located southward in comparison with the observed position of heavy rain belt which existed along the coastal zone of Pakistan. Slightly dislocated heavy precipitation center in simulation is perhaps due to northwest drift of simulated low-level jet as compared with the observed orientation.

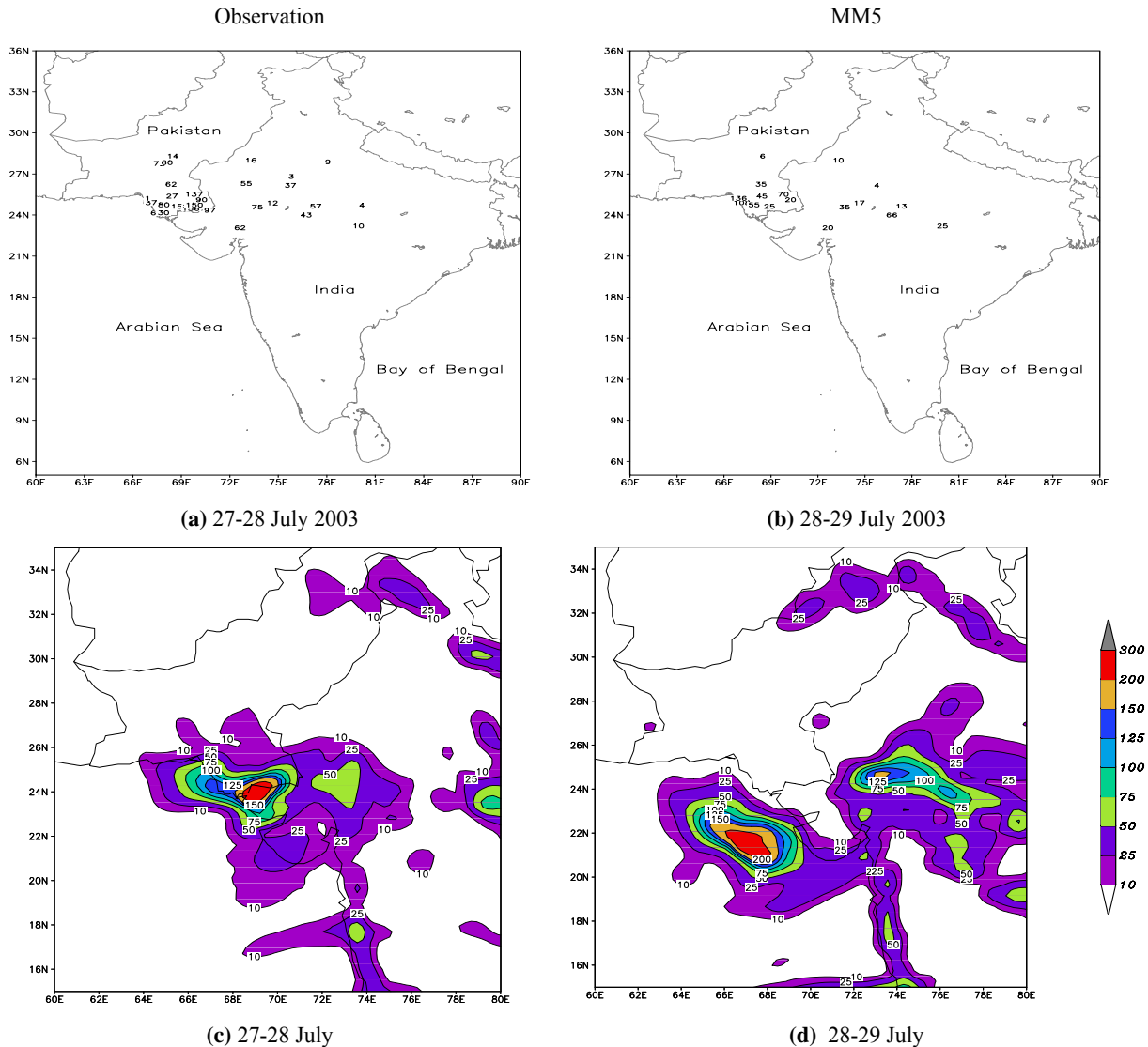


Fig10: Distribution of 24 hours total rainfall produced by MM5 at 0000UTC from 27 to 28 July 2003. The intense precipitation zone in the image is located over the coastal areas of Pakistan including Karachi on 27th July (Fig 10a) and over the Arabian Sea just south of Karachi (Fig 10b).

Summary and discussion

Based upon the above comparative analyses conducted at various temporal and spatial scales we draw following conclusions.

1. The pattern of heavy precipitation over the southern plains of Pakistan can be reproduced by non-hydrostatic meso-scale model, even though its position seems to be drifted slightly southward as compared to the observations.
2. The locations of the westerly jet at 200hPa and low-level jet at 850 hPa in south Asia are also simulated successfully. However, simulated low-level jet was stronger (about 4 ms⁻¹) than the observed one whereas the simulated westerly jet was weaker in strength by 5 ms⁻¹ as compared to observation. The center positions of maximum wind speed for westerly jet in simulation and observation perfectly coincide with each other. The position of simulated low-level jet is, however, shifted northwestward as compared to observed one, which may explain slightly dislocated heavy precipitation center in simulation toward south.
3. The simulated western portion of the Subtropical High (STH) is stronger and its location is extended far eastward over Afghanistan, which also possibly leads to the southward shift of the heavy rainfall belt.
4. The model can capture the main characteristics of the moisture flux and distribution of relative humidity during the life cycle of rain bearing system.

In general, the shift of the main rain fall belt by MM5 is caused not only by the northwestward shift of the Low-level jet or induced by the stronger and eastward extended STH, but also by the lack of water vapor in the northwest sector of Karachi. The differences of Low-level jet orientation and main precipitation centers between the observations and simulation are attributed to model's internal physical scheme including convective parameterization, the horizontal advection scheme and complex terrain features of the model domain. Overall, MM5 performed very well qualitatively to capture the system from its formation stage to heavy downpour on land even though quantitatively it showed certain deviation from the observations. Further research is needed to modify present schemes to overcome the model's limitations and to improve its quantitative abilities too.

References

1. **Bei, N.F., S. X. Zhao and S. T. Gao, 2002:** Numerical Simulation of a Heavy rainfall event in China during July 1998. *Meteorol. Atmos. Phys.* 80, 153-164.
2. **Chaudhry, Q. Z. 1991:** Analysis and seasonal prediction of Pakistan Summer Monsoon. Ph. D. dissertation at University of Philippines.
3. **Collier, C. G. 1990:** Assessing and forecasting extreme rainfall in the United Kingdom. *Weather*, Bracknell, England, 45(4): 103-112, April 1990.
4. **Das, S., J. Dudhia, D. M. Barker and M. Moncrieff, 2003:** Simulation of a heavy rainfall episode over the west coast of India using analysis nudging in MM5. Thirteenth PSU/NCAR Mesoscale Model User's Workshop, 2003.
5. **Ding, Yihui, 1991:** Advanced Synoptic Meteorology, China Meteorological Press, and 792pp.
6. **Fu C. B., H. L. Wei, M. Chen, S. B. Kai, Z. Ming and W. Z. Zheng, 1998:** Simulation of the evolution of Summer Monsoon rainbelts over eastern China from regional climate model. *Chinese Journal of Atmospheric Sciences*, 22(4), 522-534.
7. **Gao S.T, T. Lei, and Y.S. Zhou 2002:** Moist Potential Vorticity Anomaly with Heat and Mass Forcings in Torrential Rain Systems , *Chinese Physics Letters* , 19 (6) , 878-880

8. **Gao, S.T., X.P. Cui, Y.S. Zhou, and X.F. Li, 2005a:** Surface rainfall processes as simulated in a cloud-resolving model , Journal of Geophysical Research , 110, D10202 , doi:10.1029/2004JD005467
9. **Gao, S.T., X.P. Cui, Y.S. Zhou, X.F. Li, and W.-K. Tao, 2005b:**A modeling study of moist and dynamic vorticity vectors associated with two-dimensional tropical convection , Journal of Geophysical Research , 110, D17104 , doi:10.1029/2004JD005675
10. **Gao, S.T., L.K. Ran, and X.F. Li, 2006:** Notes and Correspondence: Impacts of ice microphysics on rainfall and thermodynamic processes in the tropical deep convective regime: A 2D cloud-resolving modeling study. , Mon. Wea. Rev. , 134 , 3015- 3024.
11. **Gates, W. L., 1992:** The atmospheric model inter-comparison project. Bull. Amer. Meteor. Soc., 73, 1962-1970.
12. **Harnack, R.P., D.T. Jensen and R.J. Cermak, 1998:** Investigation of upper-air conditions occurring with heavy summer rain in Utah. International Journal of Climatology, Chichester, UK, 18(7): pp. 701-723.
13. **Holtstag, A. A. M., E. I. F. De Bruijin and H. L. Pan, 1990:** A high-resolution air mass transformation model for short-range weather forecasting. Mon. Wea. Rev., 118, 1561-1575.
14. **Kulkarni, A. K., B.N. Mandal and R.B. Sangam, 1996:** Analysis of severe rainstorms over Gujarat and Punjab during the 1993 monsoon. International Journal of Climatology, Chichester, UK, 16(1): 35-47, January 1996.
15. **Mak, M.K., 1975:** The monsoonal mid-tropospheric cyclogenesis. J. Atmos. Sci., 32, 2246-2253.
16. **Ohsawa, T., H. Ueda and T. Hayashi, 2001:** Diurnal Variations of Convective Activity and Rainfall in Tropical Asia. J. of Met. Soc. Of Japan, Vol.79, No.1B, pp.333-352,2001.
17. **Pearce, R. P. and U. C. Montanty, 1984:** Onset of the Asian summer Monsoon 1979-1982. J. of Amr. Soc. 41, 1620-1639.
18. **Rajkumar, G., R. Narasimha, S.P. Singal and B.S. Gera, 1996:** Thermal and wind structure of the monsoon trough boundary layer. Proceedings, Bangalore, India, 105(3): 325-341, September 1996.
19. **Rao, Y.P., V. Srinivasan and S. Raman, 1970:** Effect of middle latitude westerly systems on Indian Monsoon. Syp. Trop. Met. Hawaii. PP. N, IV 1-4.
20. **Waterfall, P. F., 1982:** Where will the heavy rain occur? A study of the heavy rain in Northamptonshire on 26 July 1980. Meteorological Magazine, Bracknell, Eng., 111(1316): 58-67.
21. **Woodley, M. R., 1981:** Synoptic aspects relating to the development of widespread heavy rainfall over southern England on 30 May 1979. Meteorological Magazine, Bracknell, Eng., 110(1309): 207-220.
22. **Yang, S., Ki-Ryong Kang, X.P.Cui, and H.J.Wang, 2008:** Diagnostic analysis of the asymmetric structure of the simulated landfalling typhoon “Haitang”. Progress in Natural Science. 18, 1249-1260.
23. **Zhang, H. and Y. Fuquan, 1997:** Separation of different scale weather systems in heavy rain and their interaction. Geophysics, vol.33, No.1 pp. 77-84.
24. **Zeng, Q. C., B. L. Zhang, Y. L. Liang and S. X. Zhao, 1994:** East Asia Summer Monsoon-a case study. Proc. Indian Nat. Sci. Acad., 60a No. 100, 81-96.

25. **Zeng, Q.C. and J.P. Li, 2002:** On the Interaction between Northern and Southern Hemispheric Atmospheres and the Essence of Tropical Monsoon. *Chinese J. of Atmos. Sci.*, 26(3), 207-226.
26. **Zhao, S.X., N. F. Bei, J. H. Sun, H. Chen, F. Zhang and L. X. Qi, 2002:** A study of heavy rainfall systems in mid-lower latitude zone of Asian-Australian Monsoon Area. *Climate and environmental Research*, Vol.7, No.4, 377-385.